An 11-point time course midgut transcriptome across 72 h after bloodfeeding provides detailed temporal resolution of transcript expression in the arbovirus vector, *Aedes aegypti*

Hitoshi Tsujimoto and Zach N. Adelman

Genome Res. 2023 33: 1638-1648 originally published online October 6, 2023
Access the most recent version at doi:10.1101/gr.277808.123

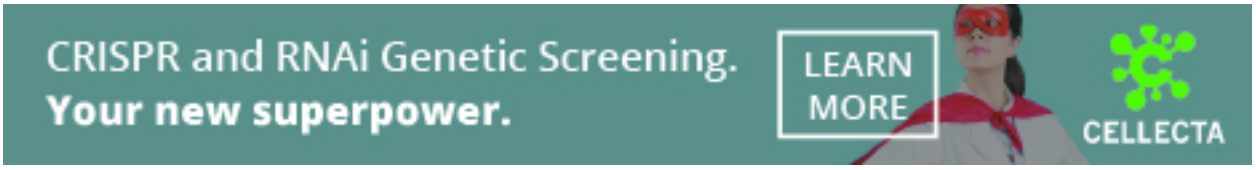

Resource

An 11-point time course midgut transcriptome across 72 h after bloodfeeding provides detailed temporal resolution of transcript expression in the arbovirus vector, *Aedes aegypti*

Hitoshi Tsujimoto and Zach N. Adelman

Department of Entomology and Texas A&M Agrilife Research, College Station, Texas 77853, USA

As the major vector for dengue, Zika, yellow fever, and chikungunya viruses, the mosquito *Aedes aegypti* is one of the most important insects in public health. These viruses are transmitted by bloodfeeding, which is also necessary for the reproduction of the mosquito. Thus, the midgut plays an essential role in mosquito physiology as the center for bloodmeal digestion and as an organ that serves as the first line of defense against viruses. Despite its importance, transcriptomic dynamics with fine temporal resolution across the entire digestion cycle have not yet been reported. To fill this gap, we conducted a transcriptomic analysis of *A. aegypti* female midguts across a 72-h bloodmeal digestion cycle for 11 time points, with a particular focus on the first 24 h. PCA analysis confirmed that 72 h is indeed a complete digestion cycle. Cluster and GO enrichment analysis showed the orchestrated modulation of thousands of genes to accomplish the midgut's role as the center for digestion, as well as nutrient transport with a clear progression with sequential emphasis on transcription, translation, energy production, nutrient metabolism, transport, and finally, autophagy by 24–36 h. We further determined that many serine proteases are robustly expressed as if to prepare for unexpected physiological challenges. This study provides a powerful resource for the analysis of genomic features that coordinate the rapid and complex transcriptional program induced by mosquito bloodfeeding.

[Supplemental material is available for this article.]

Arthropod-borne (arbo-) viruses impose a substantial burden on public health (WHO 2009, 2016, 2018, 2019). As the major vector of the dengue, Zika, yellow fever, and chikungunya viruses, the mosquito *Aedes aegypti* plays a leading role in arbovirus transmission. Transmission of these viruses occurs during bloodfeeding, which is required for reproduction of the mosquito. An *A. aegypti* female may take ~2.5 mg of blood, which is ~219% of its body weight (Stobbart 1977), and produce 60–150 eggs per batch. Laboratory strains of *A. aegypti* perform this feat (from blood ingestion to maturation of ovaries) in ~72 h. In the meantime, blood-acquired pathogens can invade midgut epithelial cells despite the presence of physical and biochemical barriers, replicate, and disseminate throughout the body of the mosquito, including the salivary glands from which the pathogens will be injected into a new vertebrate host at the next bloodfeeding. Thus, the female midgut is one of the most important organs in a mosquito as the center for bloodmeal digestion, which is directly related to reproduction and the first line of defense against blood-acquired pathogens.

Therefore, a detailed understanding of midgut physiology and the underlying genetic basis for major aspects of digestion and reproduction should provide extremely valuable knowledge to help identify novel avenues of preventing pathogen transmission or of killing bloodfeeding mosquitoes. Among many methods, transcriptomic approaches provide a global view of expressed genes in a tissue or organism, which has been useful to determine previously unrecognized genes to exploit for novel control strategies. Previous studies of the *A. aegypti* midgut transcriptome showed that the midgut undergoes very complex control of gene expression in response not only to bloodmeal but also to pathogens, which may be present in the bloodmeal (Bonizzoni et al. 2012a,b). Recent studies have added spatial resolution to the female midgut transcriptome. Hixson et al. (2022) revealed that subsections of the midgut represent quite different transcriptome profiles, and another study using single-nuclei RNA-seq uncovered that the midgut is composed of at least 20 different cell types (Cui and Franz 2020). Moreover, Raquin et al. (2017) analyzed individual midgut RNA-seq to determine host factors important for dengue virus (DENV) replication, which added resolution at individual level.

A female *A. aegypti* undergoes dynamic physiological change in response to a bloodmeal. For instance, ~24% of the bloodmeal weight will be excreted as urine within 30 min after ingestion (Stobbart 1977). Formation of the peritrophic matrix (PM), an extracellular layer that forms around the bloodmeal to protect midgut epithelium and consists of chitin and associated proteins, also occurs rapidly: A structure stained by azan (a stain for fibrous connective materials) began to form between the midgut epithelium and bloodmeal at 50 min postbloodmeal (PBM) (Freyvogel and Staeubli 1965), whereas expression of two major PM proteins (peritrophins) have been induced within 5 h after bloodmeal uptake (Shao et al. 2005; Devenport et al. 2006). Although the midgut is

Corresponding author: zachadel@tamu.edu
Article published online before print. Article, supplemental material, and publication date are at https://www.genome.org/cgi/doi/10.1101/gr.277808.123.

33:1638–1648 Published by Cold Spring Harbor Laboratory Press; ISSN 1088-9051/23; www.genome.org

expected to play a major role in such physiological changes, prior studies to date have covered only a few time points, which were mostly relevant to virus infection cycle (extrinsic incubation period of DENV: 6.5 to 15 d at 30°C and 25°C, respectively) (Chan and Johansson 2012): 5 h reported by Bonizzoni et al. (2011); 1, 4, and 14 d reported by Bonizzoni et al. (2012a); 1 and 4 d reported by Raquin et al. (2017); and 4–6, 24, 48 h (of the "gut" including crop, midgut and hindgut) reported by Hixson et al. (2022). One study analyzed a 72-h time course over five time points (0, 3, 12, 24, 72 h PBM) using hybridization-based microarray technology (Sanders et al. 2003). However, the number of genes it could analyze (predetermined 1778 genes) was far from that of modern sequencing-based technologies in quantity and quality, which makes a fair comparison unreasonable. Thus, the precise timing of changes in the midgut transcriptome over the course of bloodmeal digestion, especially within 24 h, remains largely unexplored.

To fill the gap and to uncover the breadth of dynamic change in the transcriptome throughout the digestion cycle, we conducted a transcriptomic study for 11 time points across 72 h upon bloodfeeding, which should serve as a platform for planning experiments on *A. aegypti* bloodmeal digestion and reproductive physiology at genetic and genomic viewpoints. Such studies will stimulate further advancement of *A. aegypti* research.

Results

Morphology of midgut during the time course

We captured images of the midgut with associated organs (Malpighian tubules, hindgut, and ovaries) (Fig. 1; Supplemental Fig. S1). These images depict a midgut digestion cycle (prebloodmeal and from uptake of a bloodmeal to complete clearance of the midgut) that takes 48–72 h, supporting the idea that our time course should provide a fairly complete view of the change in transcript expression throughout the digestion cycle.

Sequencing experiments

We used a laboratory strain of *A. aegypti* "Liverpool," which has a long history of usage in research and is a reference strain for the genome sequencing (Kuno 2010; Matthews et al. 2018). For the experiments for transcriptome sequencing, we used citrated sheep blood instead of defibrinated sheep blood, as the latter is not whole blood, and we considered that the response of the mosquitoes may be more natural with whole blood (such as citrated blood). We performed dissection of the midguts at the 11 time points for light cycle–matched female mosquitoes (30 midguts per time point for a replicate). To verify the consistency of each experiment, we replicated the experiment independently four times. RNA extraction, library prep, and Illumina sequencing are detailed in the Methods.

RNA-seq output and mapping

From our four independent replicates for the 11 time points of prebloodmeal and PBM, Illumina NovaSeq 6000 paired-end sequencing generated 1,160,607,602 fragment pairs (2,321,215,204 reads). We obtained a mean of 26,377,445.5 fragments per sample (ranging from 19,503,828 to 34,008,005 fragments) and 105,509,782 fragments per time point. We mapped these fragments using HISAT2 (ver. 2.1.0) (Pertea et al. 2016) onto the AaegL5 AGWG genome assembly (obtained from VectorBase) (Giraldo-Calderón et al. 2015; Matthews et al. 2018; https://vectorbase.org/vectorbase/app) with a 78.48% average mapping rate (Supplemental Fig. S2).

Through quantification of expression by StringTie (ver. 2.0) (Pertea et al. 2016), we detected 16,535 genes with nonzero transcripts per million (TPM) values in the midgut, of which 13,162 were protein-coding genes (89.4% of total in the genome), 3134 were noncoding RNA genes (66.6%), and 260 were pseudogenes (68.0%) from the current gene annotation (AaegL5.3).

Principal component analysis

As a process of validation for consistency of the replicates and changes in gene expression between time points, we performed principal component analysis (PCA) by DESeq2 (ver. 1.34.0) (Fig. 2; Love et al. 2014). PCA showed that the four replicates at all the time points were reasonably clustered, suggesting consistency between experiments. The expression changes across the time points showed a circular trace. We observed 392 genes that were differentially expressed even within <1 h PBM compared with the prebloodfed control (by DESeq2) (Supplemental Table S1). We term it as <1 h PBM for simplicity, but it was in fact ~15–20 min after bloodfeeding (see Materials and Methods), which suggests that the response of the female midgut to a bloodmeal is rapid. The difference between <1 and 4 h PBM appeared to show the largest difference between time points (5115 genes, the highest number between neighboring time points, Supplemental Table S2), which also suggests a rapid change in transcription in the first 4 h. The time points that showed the greatest difference from the prebloodmeal state (0 h PBM) were 18–24 h PBM, and the expression profile turned to near 0 h PBM at 72 h PBM (Fig. 2).

Time course analysis and Mfuzz soft clustering

Through edgeR (ver. 3.36.0) (Chen et al. 2016) time course analysis, 8594 genes showed significant change at FDR < 0.05. These genes were clustered by Mfuzz (2.54.0) (Futschik and Carlisle 2005) into 20 clusters, which were manually consolidated into

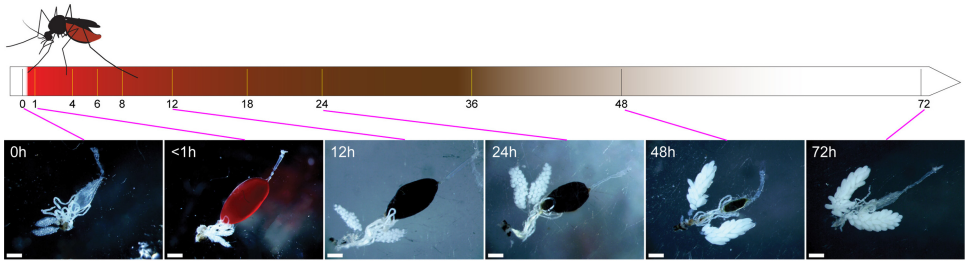

Figure 1. Time line for the midgut transcriptome sample collection time points with images of the gut system and ovaries for selected time points. Images of all the time points are shown in Supplemental Figure S1. Scale bar (white bar in each panel), 500 μm.

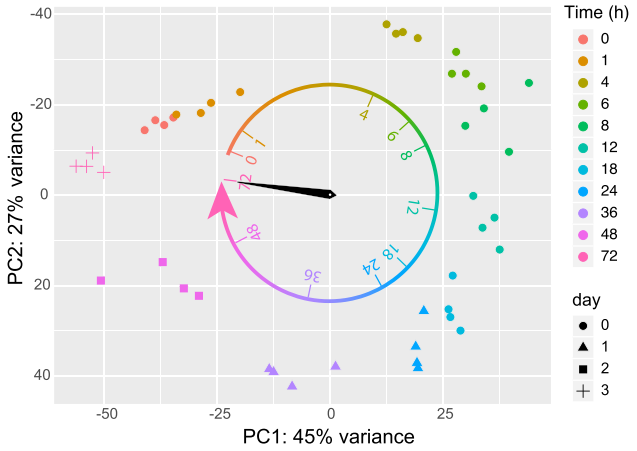

Figure 2. Principal component analysis (PCA) of the libraries. Time points (hours PBM) are shown by the color scheme and the point shapes. The circular arrow with a clock hand indicates a 72-h cycle.

13 groups by similar expression patterns, which were named by the expression peaks and bottoms: (1) 4-h peak, (2) 6-h peak, (3) 8-h peak, (4) 12-h peak, (5) 18- to 24-h peak, (6) 24- to 36-h peak, (7) 36-h peak, (8) 48-h peak, (9) up (consistently elevated expression relative to prebloodmeal state), (10) 6-h bottom, (11) 18-h bottom, (12) 48-h bottom, and (13) down (Supplemental Fig. S3).

Gene Ontology (GO) enrichment analyses using the analysis tool in the VectorBase website (Giraldo-Calderón et al. 2015), with a primary focus on "biological process" (BP) terms, indicated a far greater numbers of terms enriched in the first three peak groups (Fig. 3; Supplemental Table S2).

The general trend of enriched terms for the peak groups showed the transitioning roles of the midgut as the center for bloodmeal digestion (Fig. 4; Supplemental Table S2). The 4-h peak group was enriched with GO terms for RNA metabolism, transcription, and translation, reflecting activation of transcription and protein synthesis. The largest change between time points shown in the PCA (1–4 h PBM) (Fig. 2) may be owing to this activation of transcription and translation, which suggests the female mosquito undergoes a drastic shift in their physiology to a digestion/reproduction state. The 6-h peak group was found to be enriched with GO terms for translation (and protein synthesis), suggesting the system further shifted to protein production to deal with the bloodmeal. The 8-h peak group was enriched with GO terms related to energy production, especially oxidative metabolism, suggesting a response to the high demand for energy needed to complete digestion. The 12-h peak group was enriched with GO terms for a variety of metabolic processes such as lipid, carbohydrate and amino acid metabolism, oxidoreductase activity, and energy production, which are a potential reflection of the most active time for bloodmeal digestion. The 18- to 24-h peak group was enriched with GO terms for the regulation of cytoskeleton (mainly actin) and transport, implying that the midgut is arranging the cellular components to allocate the nutrients from the bloodmeal. The 24- to 36-h peak group was enriched with GO terms associated with autophagy, suggesting recycling and regeneration of cellular components for recovery may be at the transition of active digestion phase and recovery/regeneration phase. Although the 36-h peak group was enriched with GO terms for oogenesis and reproduction, the genes represented by these terms were composed of heme peroxidases (HPXs) and peptide hormone precursors, one of which is trypsin modulating oostatic factor (TMOF) (Borovsky 2003), which reduces the expression of trypsin in the midgut and, in turn, reduces oocyte maturation, suggesting a negative regulation of digestion in the midgut at the end of digestion, likely to shut down digestive processes. HPXs may act to suppress the midgut microbiome that had expanded upon bloodmeal, as HPXs mosquitoes appear to have immune functions (Kumar et al. 2010; Barletta et al. 2019). The 48-h peak group was enriched with the genes with metal (mostly zinc ion) binding function and nucleic acid binding ("molecular function" terms) (see Supplemental Table S2), which suggests modifying transcription by variety of DNA-binding proteins (transcription factors, enhancers, silencers, repressors, chromatin-modifying proteins, etc.). The "up" group was enriched with GO terms related to transport activity and ubiquitin-related functions, suggesting transport and protein turnover are important throughout the cycle as a hub for nutrients from the bloodmeal, implying the midgut as the center not only for digestion but also for distribution. In addition, terms related to transport are present in other peak groups (Fig. 3; Supplemental Table S2), which also suggests that transport of nutrients is important in the midgut. The down-regulated gene groups (i.e., "bottom" groups) were enriched with GO terms similar to some peak groups, such as RNA metabolism (18-h bottom, as in 4-h peak), translation (48-h bottom, as in 4-h peak and 6-h peak), and reproduction (down, including peroxidases as in 36-h peak). The 6-h bottom group contained several terms with "regulation of" (Supplemental Table S2), which implies turning off the negative regulators of many biological processes. This may be owing to role switch for the genes that have similar functions (genes for resting state vs. active digestion state).

Serine proteases

To highlight the utility of the temporal resolution provided by this data set, we focused initially on a group of genes that have a key role in blood digestion and for which there exists substantial prior work: serine proteases (SPs). With the midgut's central role for bloodmeal digestion, SPs like trypsins and chymotrypsins have

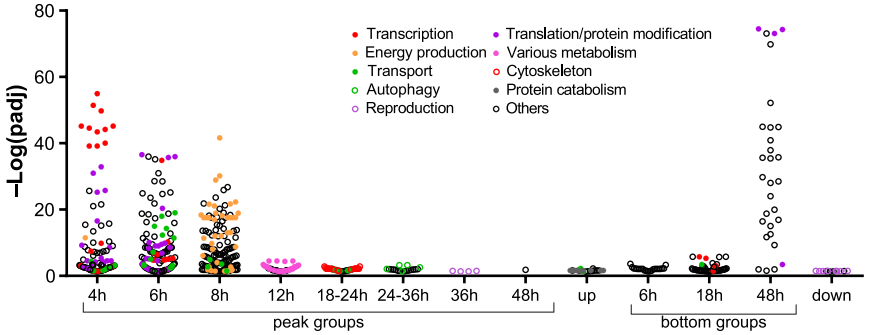

Figure 3. –log plot of Benjamini–Hochberg-adjusted *P*-values ($P < 0.05$) for GO enrichment analysis (biological process) for each cluster. Colors are applied for the related terms discussed in the text; for example, red-filled circles are GO terms related to transcription.

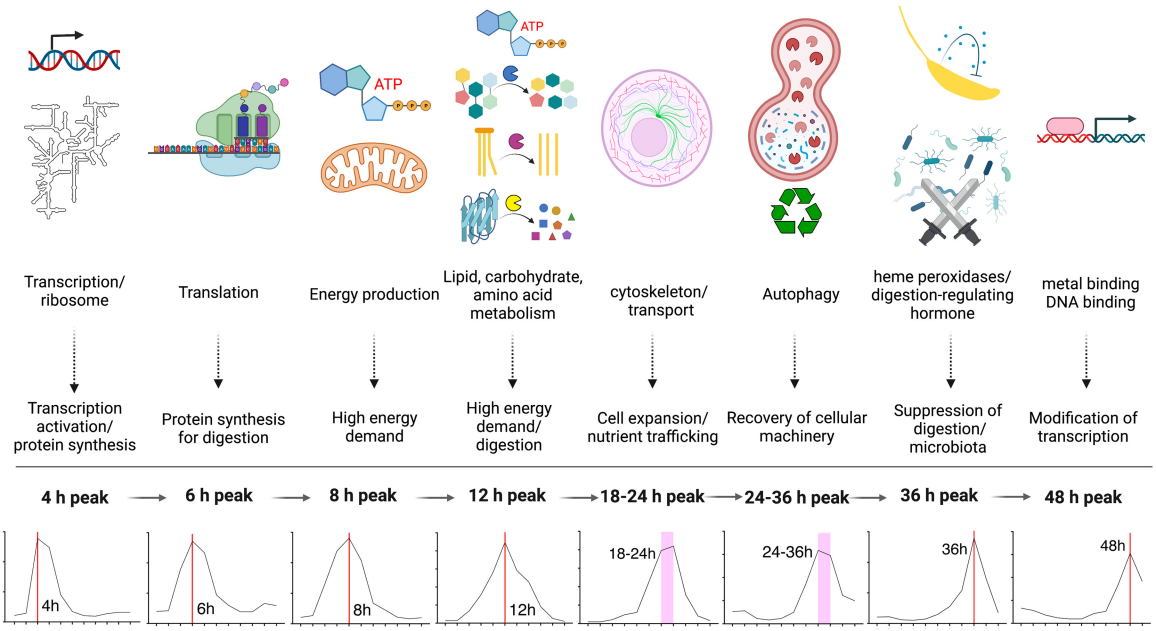

Figure 4. GO enrichment for the peak cluster groups (groups 1–8). The descriptions *below* the graphics are directly related to the top GO terms. The description *below* the arrows contains inferred roles. Created with BioRender (https://www.biorender.com).

been described to play important roles in bloodmeal digestion in the midgut (Isoe et al. 2009). Indeed, throughout the time course, eight out of the top 10 most abundantly expressed genes were SPs (Table 1), underscoring their importance in digestion.

The top highly expressed gene, AAEL003060 (adult, female-specific chymotrypsin, AaCHYMO), showed very high transcript levels with a slight reduction trend over time (Fig. 5), consistent with the observation by Jiang et al. (1997) that the expression of this protein is under post-transcriptional control. The expression patterns of the early trypsin (AaET, AAEL007818) and the late trypsin (AaLT, AAEL013284) mirror each other, providing a more detailed view of the kinetics of the temporal compartmentalization of these major enzymes (Fig. 5). Although AaET transcripts were highest at 0 h PBM (prebloodfed) and <1 h PBM, Isoe et al. (2009) described that the protein was detected only at 3–6 h PBM, suggesting post-transcriptional regulation occurs with this gene as well. AaLT transcript peaked at 24 h PBM, which corresponds the known protein expression pattern (Isoe et al. 2009). The top 10 list also includes a previously uncharacterized SP gene, AAEL001690. Expression of this gene is highly induced in response to a bloodmeal with a peak at 12–18 h PBM (Fig. 5). Carboxypeptidase A (CPA), whose promoter has been the most widely used for midgut-specific transgene expression studies, is included for comparison.

To get a comprehensive view of SPs expressed in the midgut, we obtained a list of all genes with the ontology term GO:0008236 (serine-type peptidase activity) in the *A. aegypti* genome at VectorBase. Out of 372 genes, we detected the expression of 346 genes in the midgut time course transcriptome with nonzero TPM values (Supplemental Table S3), representing 93% of the SPs. However, because many of these genes showed very low expression, we limited the list of genes to those with $\log_{10}(\text{TPM}+1) > 1.5$ for at least one time point, which reduced the number to 56. A previous study by Brackney et al. (2010) described 12 midgut SPs. Ten of the 12 genes were found in the current genome annotation (AaegL5.3) by nucleotide sequence similarity. The last two genes (AaSP II, GQ398044; AaSP V, GQ398047) appear to have been omitted owing to high nucleotide sequence similarity to AaSP III and AaSP IV, respectively, which implies that these pairs are allelic forms of the same genes or that the genes remain to be

Table 1. Top 10 most abundantly expressed genes in the midgut time course transcriptome

GeneID	Product description	ID and reference
AAEL003060	Female-specific chymotrypsin	AaCHYMO (Brackney et al. 2010)
AAEL007818	Trypsin 3A1 precursor (EC 3.4.21.4)	AaET (Isoe et al. 2009)
AAEL013284	Late trypsin 1, serine-type endopeptidase	AaLT (Isoe et al. 2009)
AAEL001703	Juvenile hormone-regulated chymotrypsin-like SP	AaJA15 (Brackney et al. 2010)
AAEL001690	Serine-type endopeptidase	
AAEL013885	Unspecified product	
AAEL007432	Serine collagenase 1 precursor, putative	AaSP I (Isoe et al. 2009)
AAEL010196	Trypsin	AaSP VI (Isoe et al. 2009)
AAEL010202	Trypsin	AaSP VII (Isoe et al. 2009)
AAEL004798	Mucin-like peritrophin	AeIMUC1 (Rayms-Keller et al. 2000)

GeneIDs in bold font are serine proteases. Product descriptions are from VectorBase.

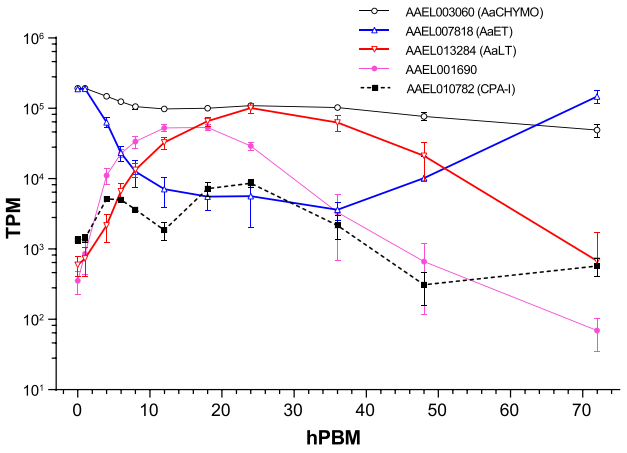

Figure 5. Expression of chymotrypsin (AaCHYMO, AAEL003060), early trypsin (AaET, AAEL007818), late trypsin (AaLT, AAEL013284), AAEL001690, and carboxypeptidase-I (AAEL010782, CPA-I, which is not a serine protease [SP]). Error bars: SD.

found in the genome. Analysis of the expression patterns shows the presence of additional SPs that have expression patterns similar to those previously described (Fig. 6). For example, AaLT (AAEL013284) shows a peak ~18–36 h PBM and the lowest at the 0–1 h PBM (as well as 72 h PBM). There are 11 other genes that show similar expression patterns (peak at 18–36 h PBM with lowest at 0 or 72 h PBM) (Fig. 6, orange shading), including some previously studied genes (AaSP VI, AaSP VII, and Aa5G1) and eight additional genes (also AAEL001690 discussed above) (Fig. 6, orange shading), which may cooperatively participate in bloodmeal digestion. AaSP I (AAEL007432) shows elevated expression at earlier time points and remained high [$\log_{10}(\text{TPM}+1) > 4$] between 4 and 18 h PBM. There were five additional genes that show similar expression patterns (Fig. 6, purple shading), which may be important in the initial digestion phase. Finally, there were also SP genes with an expression peak at later time points (36–48 h PBM) (Fig. 6, blue shading), suggesting potentially different roles in digestion. Thus, this study expands the existing knowledge about SPs in the midgut in context of the bloodmeal digestion physiology.

A previous study indicated that targeting specific SPs by RNAi can slow digestion and reduce fecundity (Isoe et al. 2009). To confirm these results and investigate the role of these new SPs, we injected dsRNA targeting one or more SPs and evaluated the effects on reproductive output. We selected highly expressed SP genes in response to a bloodmeal, along with AaCHYMO, the most highly expressed gene, for two groups: (1) the genes previously studied and showing reduced reproductive fitness by RNAi (AAEL013284 [AaLT] and AAEL010196/AAEL013712 [AaSP VI/5G1; these genes were targeted/analyzed together as the sequences are nearly identical]; AAEL010202 [AaSP VII]) (Isoe et al. 2009) and (2) AAEL001690, AAEL3060 (AaCHYMO), and AAEL007432 (AaSPI), genes that had not been previously characterized. Although we observed robust silencing of transcripts at 24 h PBM (Supplemental Fig. S4) for all targeted genes, we did not observe any differences in fecundity (egg numbers) or fertility (hatch rates) (Supplemental Fig. S5).

Iron/heme-related genes

Previously, we conducted screens for putative iron transporters (Tsujimoto et al. 2018, 2021), PM proteins (Whiten et al. 2018), and putative heme transporters (Eggleston and Adelman 2020) to better understand iron/heme handling from a bloodmeal in *A. aegypti*. Using a list of those genes along with ferritins, transferrins, and recently determined heme exporters (Wang et al. 2022), we analyzed expression across our midgut transcriptome time course (Supplemental Table S4).

Putative iron transporters

Within the ZnT and ZIP family putative iron transporters (Fig. 7, blue shading), AaeZIP13 showed elevated expression that peaked at 24 h PBM (Fig. 7), consistent with our previous observation

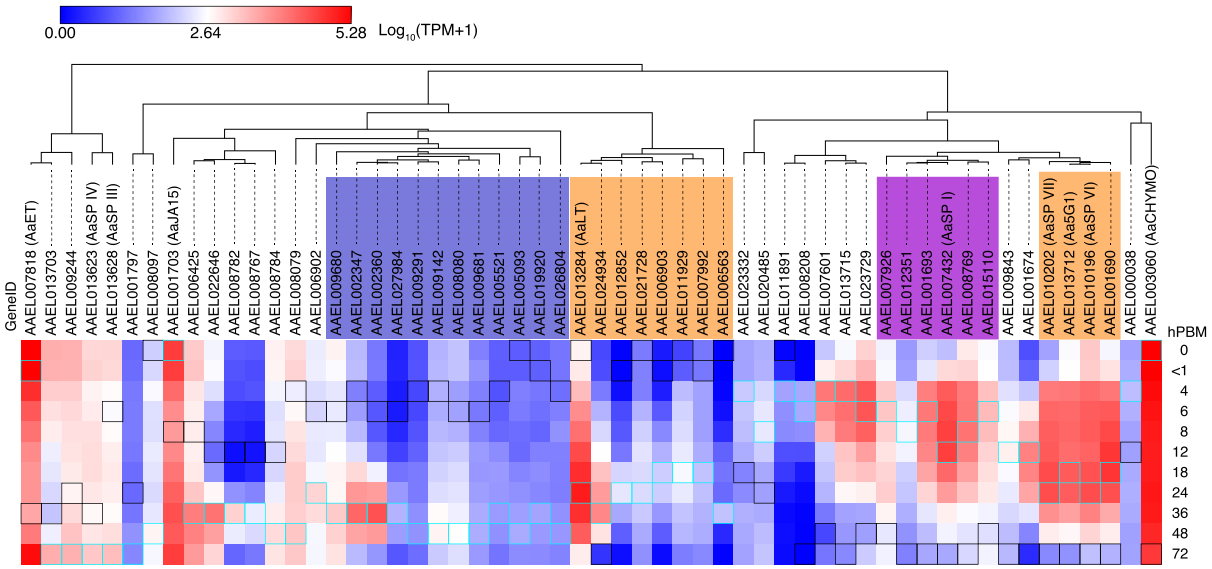

Figure 6. Expression patterns of SPs with $1.5 < \log_{10}(\text{TPM}+1)$ at least one time point. Genes were hierarchically clustered by expression patterns. Maximum and minimum values across the time course are indicated by cyan and black squares, respectively. For the groups indicated by colored shadings, see text.

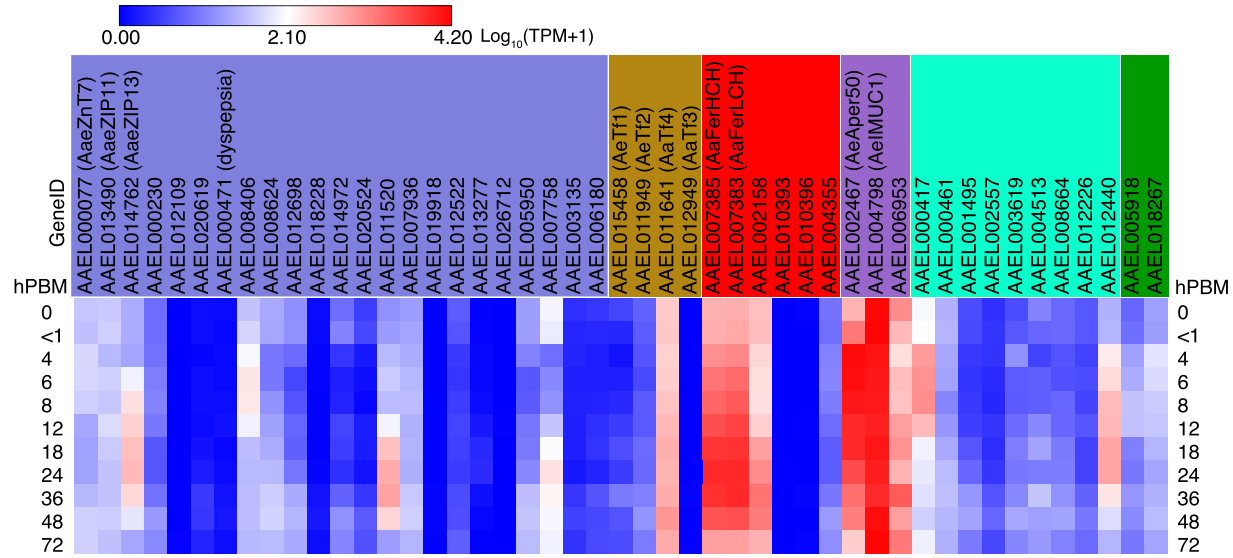

Figure 7. Heat map showing expression patterns of putative iron transporters (blue shading), transferrins (brown shading), ferritins (red shading), peritrophins (lavender shading), putative heme transporters (cyan shading), and verified heme exporters (green shading). The genes that showed no expression across all the time points were excluded. See also Supplemental Table S4.

(Tsujimoto et al. 2018). AaeZnT7 and AaeZIP11 showed relatively lower expression without drastic changes to transcript abundance across the time points, with just a moderate increase at ~6 h PBM, 48–72 h PBM for AaeAZnT7, and 12 and 48 h PBM for AaeZIP11. Among the genes identified in a screen for putative iron transporters, three (AAEL008406, AAEL011520, and AAEL007758) showed a TPM higher than 100 (Fig. 7, white to shades of red; Supplemental Table S4). Of these, AAEL008406 (annotated as a cationic amino acid transporter) displayed a peak of expression at ~6–8 h PBM, whereas AAEL011520 (SLC45/sugar transporter) and AAEL007758 (unknown function) showed peak expression at ~24–36 h PBM (Fig. 7; Supplemental Table S4).

Transferrins

Transferrins (Tfs) (Fig. 7, brown shading) are known to be multifunctional iron-binding proteins (Zhou et al. 2009). Four transferrin genes are present in the *A. aegypti* genome, among which two (AaTf1 and AaTf2) have been functionally studied. AaTf1 transcripts were found in fat bodies and adult female thorax, which were elevated by bloodmeal and bacterial challenge in the ovaries (Harizanova et al. 2005; Zhou et al. 2009). AaTf1 protein was also found in the hemolymph (Harizanova et al. 2005). AaTf2 transcripts are found in fat bodies and ovaries with suggested functions in development and wound response (Zhou et al. 2009). Here, we show that unlike AaTf1-3, AaTf4 (AAEL011461) was highly expressed in the midgut (Fig. 7; Harizanova et al. 2005; Zhou et al. 2009). Functional study on AaTf4 may uncover the role of AaTf4 in iron transport and control of gut microbiota upon bloodmeal.

Ferritins

Ferritins (Fig. 7, red shading) in general are known to be multimeric proteins that make a large sphere to cage thousands of Fe^{3+} (Pham and Winzerling 2010). Unlike mammalian ferritins, which serve as iron storage proteins, insect ferritins are considered to function as iron shuttle proteins and protectants from oxidative damages caused by ferrous ammonium sulfate (Fe^{2+}) (Pham and Winzerling 2010). The *A. aegypti* genome contains seven ferritin-like genes, of which no transcript for AAEL000359 was detected in the midgut transcriptome (Supplemental Table S4). In *A. aegypti*, ferritin light chain (FerLCH, AAEL007383) and heavy chain (FerHCH, AAEL007385) are well documented. Both proteins have been shown to be induced by a bloodmeal in the midgut (Dunkov et al. 2002). Transcripts of the two genes were induced by Fe^{2+}, hemin (heme-related compound), and H_2O_2 in whole bodies (Geiser et al. 2003). As expected, the most highly expressed ferritin genes in the midgut were AAEL007383 and AAEL007385 (Fig. 7). These genes are closely located by head-to-head orientation, which was determined to contain multiple transcription start sites and documented FerLCH and FerHCH promoters (Geiser et al. 2003; Pham et al. 2003; Pham and Chavez 2005). The expression patterns and levels of these genes are nearly identical, which supports the idea that these genes are operated by a common promoter. Their increased expression after a bloodmeal may be a response to elevated iron levels to mitigate the oxidative damage by Fe^{2+}. The promoter for AAEL007383 (AaFerLCH) was shown to be specifically responsive to the intracellular iron levels in a cultured cell line, Aag2 (Tsujimoto et al. 2018). Another ferritin gene, AAEL002158, also shows high expression with induction at later stage (>12 h PBM) than the other two, which implies a distinct role in bloodmeal digestion.

Peritrophins

All three previously described midgut peritrophins (Fig. 7, lavender shading) were found to be highly expressed across the time course (Fig. 7). AAEL004798 (AeIMUC1) showed very high expression throughout the time course; it is indeed one of the top 10 most expressed genes (Table 1), although its transcript expression was not induced by bloodfeeding. Because it has been shown to bind a large amount of heme (Devenport et al. 2006), AeIMUC1 may be the major heme-sequestering peritrophin. AAEL006953 also showed varied expression levels across the time course. On the other hand, AAEL002467 (AeAper50) expression was highly induced

by a bloodmeal, which agrees with a previous report, although our study lacks the 2 h PBM time point, the potential true expression peak (Shao et al. 2005). The response was quite rapid; at <1 h PBM, TPM increased more than three times from 0 h PBM, reaching a peak (TPM: 13,025; 25× of 0 h PBM) at 4 h PBM and maintained at least half of the peak level until 18 h PBM (Supplemental Table S4). Protein expression of AeIMUC1 appears to be post-transcriptionally regulated and showed a peak at 4 h PBM (Devenport et al. 2006); the high transcript level before this time point may be prerequisite for the rapid production of a high amount of protein product to protect the midgut. This also implies that at least AeIMUC1 and AeAper50 orchestrate their expression for a rapid formation of PM, which precedes the major digestive phase.

Putative heme transporters

Heme (Fig. 7, cyan shading) is a component of the major blood protein, hemoglobin. Like iron, heme can cause cellular damage despite also serving as a vital nutrient and a signaling molecule in trace amounts (Eggleston and Adelman 2020). In a previous study based on cell culture transcriptomes, several transporters whose expression levels were responsive to heme were identified (Eggleston and Adelman 2020). Among these, two genes showed high (TPM greater than 100) expression (AAEL000417 and AAEL012440) (Fig. 7; Supplemental Table S4) in our midgut transcriptome time course. Gene AAEL000417 (a member of the monocarboxylate transporter family) showed a rapid increase of transcript with a peak at 6–8 h PBM, whereas AAEL012440 (annotated as sodium-bile acid cotransporter) showed a gradual increase with a peak at 18–24 h PBM. The fact that these genes respond transcriptionally both to heme exposure and to a bloodmeal in the midgut suggests potential roles in blood digestion/detoxification that remain to be determined.

Recently, a heme exporter has been characterized from *Drosophila melanogaster* (Wang et al. 2022). The same study verified that homologs in *A. aegypti* also had similar activity. The transcript expression of these genes (AAEL005918 and AAEL018267) in the midgut were not markedly high and were only mildly induced by bloodfeeding, suggesting either that very little heme is exported to the hemolymph or that there are additional heme exporters that remain to be determined that complement this function.

Comparison with Hixson et al. data

To highlight similarities and differences between this study and the recent time course transcriptome study of the gut by Hixson et al. (2022), we compared peptidase genes shown in their figure 3F and found that our results are comparable (Supplemental Fig. S6). In fact, despite the conclusion based on the PCA by Hixson et al. (2022), this result along with theirs supports 72 h as the total length of the digestive cycle. We next compared the expression patterns of eight major SPs individually (Supplemental Fig. S7). The expression patterns of these genes, in general, resemble each other between the two studies, just different in temporal resolution. Further we compared digestive enzymes and transporter genes expressed in the gut from Supplemental File 4 by their groupings: lipid digestion, lipid transporters, amylases, maltases & glucosidases, sugar transporters, peptidases, and amino acid transporters, representing by heatmaps (Supplemental Fig. S8). These showed very comparable expression patterns across multiple groups of genes between the two studies. Thus, our study provides deep temporal resolution that can be overlaid on the spatial resolution provided by Hixson et al. (2022).

Discussion

This study used Illumina sequencing technology to present the midgut transcriptome from the prebloodfeeding state to the completion of bloodmeal digestion at 72 h in 11 time points in the most important mosquito vector of arboviruses worldwide, the first study to cover a complete digestion cycle in *A. aegypti* with such fine temporal resolution. We obtained a total of more than 1 billion paired-end fragments, which provided a depth of more than 26 million fragments per sample. The PCA showed a huge transcriptomic change between <1 and 4 h PBM, which suggests that additional time points between <1 and 4 h PBM are warranted in future studies, and may fill a useful knowledge gap in understanding midgut digestion physiology. The remaining differences in gene expression between 0 (start of the cycle) and 72 h PBM (end of the cycle; 1421 genes differentially expressed) may be owing to the state of ovaries. Because we used gravid females, the midgut may require signals from nongravid ovaries to revert to the prebloodmeal state, independent of the time elapsed. Thus, the PCA analysis along with our imaging results suggests that 72 h is indeed a complete (or close to complete) cycle of blood digestion in the midgut.

Our PCA results differ from the recent results from Hixson et al. (2022), which suggested 48 h as a cycle. This discrepancy might be because this study used different strain of *A. aegypti* ("Liverpool" vs. Thai strain), source of blood (citrated sheep blood vs. live chicken), different tissue components (whole midgut vs. crop, midgut, and hindgut combined), temperature (28°C vs. 29°C), light cycle (14:10 vs. unknown), and number of time points. Moreover, the PCA between the two studies might have used different components as principal factors. However, close comparison between the two studies revealed far more similarities than differences (Supplemental Figs. S6–S8). Thus, the time course expression patterns between the two studies are reasonably similar, which suggests that the time course study of both studies is comparable, although some experimental parameters were different. This also suggests that the *A. aegypti* Liverpool strain retains major digestion physiology similar to the "near" wild strain of *A. aegypti* (the Thai strain used in the Hixson et al. study).

The clustering analysis and associated GO term enrichment analysis (Figs. 3, 4; Supplemental Fig. S3; Supplemental Table S4) showed that the midgut operates as the center for digestion (and transport) by regulating gene expression in an orchestrated manner to set the stage for the most important task for a female mosquito, reproduction. This analysis also suggested that the midgut functions as a distribution center for nutrients obtained from the bloodmeal.

The data we obtained may be used to analyze expression patterns of genes in the same functional category, such as the SPs discussed in this paper, or other categories of interest such as secreted proteins, membrane-bound transporters, or immune pathways. Our analysis of SPs has revealed a number of previously undescribed SPs that may function synergistically or have different roles in bloodmeal digestion (Fig. 6). The view of detailed temporal expression patterns helps categorize (or subcategorize) groups of genes, especially complex sets of genes. Even a familiar gene may provide us with a new insight in the context of the time-course expression, such as expression peaks that may be a component to

consider when developing a control strategy (timing of application).

To investigate the utility of the data for functional studies, we conducted RNAi on selected SPs and assessed the effects on reproductive fitness. Unlike the similar study by Isoe et al. (2009), we did not observe reductions in fecundity or fertility in the gene-silenced mosquitoes despite the huge reduction of mRNA expression. This may be because of redundancy, as in each case there were additional SPs showing similar expression patterns (orange- and lavender-shaded groups) that could compensate for the reduction of the targeted genes. Additionally, although RNAi substantially reduced transcript levels from their wild-type levels, even this residual remaining expression could have been sufficient to produce enough of the targeted protein, as suggested by their Ct values. Finally, as shown by our GO term enrichment analysis of clustered coexpressed genes, the midgut substantially increases its metabolic activity, transcription, and translation machineries upon bloodmeal acquisition (Fig. 4; Supplemental Table S3), which might also compensate for a reduction of the transcripts of the SPs. Establishing the importance of various SPs may require the generation of stable, multiplexed CRISPR-Cas9-based gene edited strains to cope with the extreme redundancy built to protect the process of bloodmeal digestion.

In addition to bloodmeal digestion, an earlier study reported that the addition of a trypsin inhibitor in a DENV-containing bloodmeal reduced viral titer in the mosquitoes (Molina-Cruz et al. 2005), suggesting the importance of SPs in susceptibility to viruses. Bonizzoni et al. (2012b) suggested that differences in susceptibility for DENV between different strains of *A. aegypti* may be related to a trypsin, particularly AAEL007818 (AaET). They detected a difference in reduction of AaET at 5 h PBM between DENV-susceptible and DENV-resistant strains (Bonizzoni et al. 2012b). However, our data suggest that SPs in the midgut microecosystem seem to be more complex, and the correlation of SPs to DENV infection and dissemination requires further investigation.

Despite the importance of the gut in both blood digestion and pathogen transmission, only two promoters have been empirically verified to date for the midgut-specific expression in *A. aegypti*: CPA-I (AAEL010782) (Moreira et al. 2000) and AaET (Zhao et al. 2016). We confirmed that the CPA-I transcript expression has two peaks at 4–6 h PBM and 24 h PBM (Fig. 5). Our observation parallels the study on transgene expressing luciferase under the CPA-I promoter, particularly luciferase transcript expression (see fig. 4 of the reference), which showed strong signal at 8 h PBM and 20–24 h PBM with a weaker signal at 12 h PBM (Moreira et al. 2000). Studies with particular interest in transgene expression in the midgut at 12 h PBM may consider avoiding the use of this promoter. AaET expression is robust prebloodmeal, but it reduced during the major digestion phase, confirming that the AaET promoter is not suitable for bloodmeal-inducible expression of transgenes. Promoters from genes like AaLT and AAEL001690, as well as the genes that showed similar expression patterns (orange groups in Fig. 6), may serve for a more robust blood meal-inducible transgene expression in the midgut. Moreover, owing to the high transcript expression, investigation of *cis*-regulatory elements (promoters) for the SPs may lead to future usage for midgut-specific transgene expression, although organ/stage-specific expression may need to be verified.

A recent study on transcriptome of all three tagmata (head, thorax, and abdomen) with a subsectioned gut system and ovaries uncovered previously understudied spatial resolution of gene expression in the female *A. aegypti* (Hixson et al. 2022). This study complements their study by providing the finest temporal resolution known to date for bloodmeal digestion cycle of *A. aegypti*, which may serve as a platform for further studies. Moreover, similar studies based on the transcriptomics of other organs with a fine time component like this should greatly enhance our understanding of physiology and genetics of bloodfeeding mosquitoes and lead to new research avenues.

Methods

Mosquitos

The *A. aegypti* Liverpool strain was maintained in an insectary at Texas A&M entomology in environmental chambers kept at 27°C, 70% RH, and 14:10 (light:dark) cycles. Immature stages were reared with ground TetraMin (Tetra), and adults were fed on defibrinated sheep blood (Colorado Serum Company).

Bloodfeeding and midgut dissection

For all the experiments, female mosquitoes 3–4 d after eclosion were used (the females were eclosed in the presence of males). They were maintained on 10% sucrose (granulated sugar from local grocery stores) in water and starved for ~16 h before bloodfeeding. Mosquitoes were fed on citrated sheep blood (Hemostat Laboratories) via an artificial membrane feeder for ~15 min and anesthetized on ice, and only engorged ones were selected for midgut collection. Midguts were dissected from 0 PBM (prebloodfed/starved, set aside when bloodfeeding was performed), <1 h PBM (no recovery from anesthesia), and 4, 6, 8, 12, 18, 24, 36, 48, and 72 h PBM. The mosquitoes were discouraged from laying eggs on the sugar source (common with 10% sucrose) by increasing the concentration to 30% sucrose. To be consistent with the mosquito's circadian rhythm, bloodfeeding was performed ~1 h after the beginning of the light cycle. Bloodmeal (bolus) was removed from the midguts upon collection. A pool of 30 midguts was collected in a 1.5-mL microcentrifuge tube with TRIzol (Thermo Fisher Scientific) and stored at –80°C for downstream processing. A total of four independent replicates were made for each time point.

RNA extraction, library prep, and sequencing

Whole RNA was extracted with a TRIzol (Thermo Fisher Scientific) standard protocol with half-volume format (0.5 mL TRIzol), and initial homogenization was in a small volume of TRIzol (20 µL) using an RNase-free pestle (Contes). RNA pellets were resuspended with 16 µL of nuclease-free H_2O and treated by DNase (2 µL of DNase buffer and 2 µL of TURBO DNase; Thermo Fisher Scientific) for 1 h at 37°C. RNA was quantified by a Qubit RNA broad range kit (Thermo Fisher Scientific). The integrity of the RNA was analyzed by a fragment analyzer (Agilent Technology).

Illumina libraries for RNA-seq were prepared using NEBNext Ultra II RNA library prep kit for Illumina (NEB E7770) with a NEBNext poly(A) mRNA magnetic isolation module (NEB E7490) and NEBNext multiplex oligos for Illumina (96 unique index primer pairs; NEB E6440). We used a 13-min fragmentation time and nine cycles of PCR enrichment on 1000 ng of total RNA input determined by preliminary library preparation. All libraries were quantified by a Qubit with dsDNA BR kit (Thermo Fisher Scientific) and quality-checked by a fragment analyzer (Agilent Technology).

Prepooling quantification by qPCR, pooling, and sequencing on a NovaSeq 6000 in a 2 × 100 bp (paired-end) format, using an

entire flowcell for all the libraries, were performed by the genomics and bioinformatics service at Texas A&M Agrilife Research.

Bioinformatics analysis

The Illumina reads were mapped, and expression was quantified using a HISAT2 (ver. 2.1.0) and StringTie (2.0) pipeline (Pertea et al. 2016) using the AaegL5 genome and AaegL5.2 gene set obtained from VectorBase (Giraldo-Calderón et al. 2015). StringTie was used with the "-e" and "-A" options. The above processes were performed using the Texas A&M high performance research computing system. A count table ("gene_count_matrix.csv") for downstream analysis (with DESeq2 and edgeR) was generated by the Python script "prepDE.py" provided in the StringTie manual online (https://ccb.jhu.edu/software/stringtie/index.shtml?t=manual). A TPM table for each library was generated from count tables generated by the -A option of StringTie, and the tables for all 44 libraries were combined into one table using a Python script. Pair-wise differential expression analyses and PCA were performed using the DESeq2 package (ver. 1.34.0) (Love et al. 2014) on R (ver. 4.1.1) (R Core Team 2023). The combined TPM table was trimmed using a Python script to remove the genes with zero values across all the time points. The final TPM table is provided as Supplemental Table S5, and the gene IDs from the list were searched on VectorBase to obtain the information on the gene types (protein-coding, noncoding, and pseudogenes).

Time course analysis was performed following an example shown in the edgeR package (on R ver. 4.1.1; ver. 3.36.0) (Chen et al. 2016) user's guide (June 2020 version), which uses smoothing spline with df = 3. Through this, we obtained a list of genes showing significant change across the time course with a false-discovery rate (FDR) < 0.05. Then using the FDR < 0.05 gene list, we performed soft clustering analysis using an R package "Mfuzz" (ver. 2.54.0) (Futschik and Carlisle 2005) to obtain gene lists with similar expression patterns. With this analysis, we generated 20 clusters by expression patterns, which were consolidated into 13 groups. GO enrichment analyses were performed for the biological process and molecular function categories using the enrichment analysis option on VectorBase (https://vectorbase.org/vectorbase/app).

The codes used for HISAT2, StringTie, DESeq2 (including PHENO_DATA.csv table), edgeR, and Mfuzz are provided as Supplemental Code.

Gut system and ovary imaging

Age-matched (to the mosquitoes used for sequencing) *A. aegypti* "Liverpool" females were bloodfed using a membrane feeder and defibrinated sheep blood. The midgut, Malpighian tubules, hindgut, and ovaries were dissected at the same time points PBM. Unlike RNA-seq samples, mosquitoes were bloodfed at different times of the day so that dissection could be performed in the working hours. The dissected organs were photographed using an AmScope MU300 digital camera (AmScope)–equipped stereo-microscope Leica M165FC. The scale bar was added by Fiji (ImageJ) (Rueden et al. 2017) using an image of a hemacytometer (Hausser scientific) grid with the same magnification as a scale reference.

SP gene family analysis

To obtain a list of SPs in the *A. aegypti* genome, we used the GO term GO:0008236 (serine-type peptidase activity) on VectorBase. The expression data were retrieved from the master expression table (in TPM) using a Python script. To filter SP with reasonable expression levels, the list was filtered to have $\log_{10}(\text{TPM} + 1) > 1.5$ for at least one time point on Microsoft Excel. To visualize the expression patterns of these genes, Morpheus (https://software.broadinstitute.org/morpheus) was used with hierarchical clustering with default parameters (one minus Pearson's correlation and average linkage). The modification of the labels and dendrogram, as well as high and low value highlighting, were performed using Illustrator (version 26; Adobe).

RNAi analysis on SP genes

Primers for amplifying dsRNA templates were designed for SPs AAEL001690 and AAEL007432 (AaSP I) using Primer-blast (Ye et al. 2012) with PCR product size to be 350–600 bp, and a 20-nt T7 promoter sequence was added at the 5′ end. The resultant dsRNA sequences were searched against the AaegL5.3 transcript set (from VectorBase) using the standalone BLAST+ program (ver. 2.13.0) (Camacho et al. 2009) with the "-word_size 19" option with no off-target detected. Primer sequences for other genes (AAEL003060, AAEL013284, AAEL010202, AAEL010196/AAEL013712) were from Brackney et al. (2008) and Isoe et al. (2009) with some modifications (using 20-nt T7 sequence and 3′ deletion for annealing temperature adjustment). Phusion HiFi DNA polymerase (New England Biolabs) was used to amplify the template DNA; the products were purified using the Nucleospin gel and PCR cleanup kit (Machery-Nagel) and quantified with NanoDrop One (Thermo Fisher Scientific). One microgram of the DNA was used as template for dsRNA synthesis using MEGAscript T7 transcription kit (Thermo Fisher Scientific) overnight at 37°C. The synthesized dsRNA was purified using a MEGAclear transcription cleanup kit (Thermo Fisher Scientific); the resulting RNA pellets were resuspended with nuclease-free water, quantified by NanoDrop One, and aliquoted for injection sessions. The dsRNA (~1 µg each target) was thoracically injected using Nanoject II (Dummond) into females within 48 h after eclosion. The females were kept with a cotton pad containing 10% sucrose solution. The cotton pads were removed ~16 h before bloodfeeding. The starved females were bloodfed using artificial feeders and defibrinated sheep blood. After 15 min of bloodfeeding, the mosquitoes were anaesthetized on ice, and only engorged ones were kept with a 30% sucrose cotton pad. Midguts were dissected at 24 h PBM (up to seven individuals) for quantification of transcript (at least for a replicate) by qRT-PCR. At 72 h PBM, the remainder were transferred to the EAgaL plates (Tsujimoto and Adelman 2021), which consisted of 24-well tissue culture plates with agarose on the well bottom for fecundity and fertility evaluation. Briefly, the females were allowed to lay eggs for 24 h and were removed from the EAgaL plates. Images of each well were captured by a compact digital camera (TG-6, Olympus) and were used for counting eggs using ImageJ (Rueden et al. 2017). Right after the well imaging, water was added to each well and monitored for hatching. Five days after oviposition, images of each well were captured for larval counting. GraphPad Prism was used for statistical analysis (Kruskal–Wallis with multiple comparison test) and graphing.

Quantitative real-time PCR (qRT-PCR) primers were designed for AAEL001690, AAEL007432, and AAEL003060 using Mfold (Zuker 2003) for secondary structure prediction (at 60°C) and Primer-blast with PCR product size to be 50–150 bp and 3′ self-complementarity "0." Other primers were taken from previous studies (Brackney et al. 2008; Isoe et al. 2009). These primers were designed for at least one primer to be outside of the dsRNA site. qRT-PCR reactions were run on a Bio-Rad CFX96 using SsoAdvanced universal SYBR Green supermix (Bio-Rad). Amplification parameters were for 30 sec at 95°C and 45 cycles of 15 sec at 95°C and 30 sec at 60°C followed by melt analysis between 65°C and 95°C. All reactions were performed in triplicate.

The amplification efficiency of the primer pairs was empirically determined using serial dilution of midgut cDNA. The percentage knockdown was calculated by the following formula: % knockdown = (1 – [normalized expression of dsEGFP/normalized expression of dsTarget]) × 100.

All the primers with their information are shown in Supplemental Table S6.

Comparison with Hixson et al. data

To show similarity and differences between this study and the study by Hixson et al. (2022), we retrieved supplemental file 4 and used the TPM values from the file. We only used whole-gut sugar-fed, 4–6 h (denoted 6), 24 h, and 48 h PBM data. TPM values for the same sets of genes were extracted from our data (Supplemental Table S1) using a custom Python script. To generate a graph similar to the figure 3F of Hixson et al. (2022), the expression data were extracted from our master TPM table (Supplemental Table S1) and the values transformed to percentage max across the time points for a better comparison using Excel. Line graphs were generated by plotting the percentage max values using GraphPad Prism. Heatmaps were generated for $Log_{10}(TPM + 1)$ values for both studies using Morpheus.

Putative iron and heme transporters, and heme-binding proteins

The genes found to have relation to iron transport were obtained from Tsujimoto et al. (2018) and from the table 1 of Tsujimoto et al. (2021). The heme transporter candidates were from the table 6 of Eggleston and Adelman (2020); heme exporters were from Wang et al. (2022). The PM proteins with chitin binding domains were from Whiten et al. (2018) (AAEL002495 is AAEL004798 in the current annotation AaegL5.3). Transferrins and ferritins were retrieved by text searches for "transferrin" and "ferritin" on VectorBase. The list of the genes is in Supplemental Table S5. The expression values (transcripts per million) for the genes were extracted from the master TPM table (Supplemental Table S1) using a Python script and $log_{10}(TPM + 1)$-transformed on Microsoft Excel. Morpheus (https://software.broadinstitute.org/morpheus) was used to visualize expression patterns after the removal of any genes that had zeros for all the time points (AAEL019992 and AAEL000359). Additional labels and markings were made using Illustrator (Adobe).

Data access

The raw sequencing reads (FASTQ.gz) generated in this study have been submitted to the NCBI BioProject database (https://www.ncbi.nlm.nih.gov/bioproject/) under accession number PRJNA639291.

Competing interest statement

The authors declare no competing interests.

Acknowledgments

Fragment analyzer quality analysis of RNA and the Illumina libraries and NovaSeq sequencing (including library quantification and pooling) were performed by the Texas A&M AgriLife genomics and bioinformatics service. Portions of this research were conducted with the advanced computing resources provided by Texas A&M High Performance Research Computing. We also thank Emma Jakes, Kristen Gilbert, and undergraduate research associates for helping with rearing, bloodfeeding, and dissecting mosquitoes and Cara Muenzler for assistance for fecundity and fertility analysis (EAgaL plate assay). This work was funded by the USDA National Institute of Food and Agriculture, Hatch project 1018401, and by Texas A&M AgriLife Research under the Insect Vectored Disease Grant Program to Z.N.A.

Author contributions: H.T. conceived, designed, and conducted the project; analyzed and managed the data; and wrote and revised the manuscript. Z.N.A. assisted with the experimental design and data analysis pipeline development and revised the manuscript.

References

Barletta ABF, Trisnadi N, Ramirez JL, Barillas-Mury C. 2019. Mosquito midgut prostaglandin release establishes systemic immune priming. *iScience* **19:** 54–62. doi:10.1016/j.isci.2019.07.012

Bonizzoni M, Dunn WA, Campbell CL, Olson KE, Dimon MT, Marinotti O, James AA. 2011. RNA-seq analyses of blood-induced changes in gene expression in the mosquito vector species, *Aedes aegypti*. *BMC Genomics* **12:** 82. doi:10.1186/1471-2164-12-82

Bonizzoni M, Dunn WA, Campbell CL, Olson KE, Marinotti O, James AA. 2012a. Complex modulation of the *Aedes aegypti* transcriptome in response to dengue virus infection. *PLoS One* **7:** e50512. doi:10.1371/journal.pone.0050512

Bonizzoni M, Dunn WA, Campbell CL, Olson KE, Marinotti O, James AA. 2012b. Strain variation in the transcriptome of the dengue fever vector, *Aedes aegypti*. *G3 (Bethesda)* **2:** 103–114. doi:10.1534/g3.111.001107

Borovsky D. 2003. Trypsin-modulating oostatic factor: a potential new larvicide for mosquito control. *J Exp Biol* **206:** 3869–3875. doi:10.1242/jeb.00602

Brackney DE, Foy BD, Olson KE. 2008. The effects of midgut serine proteases on dengue virus type 2 infectivity of *Aedes aegypti*. *Am J Trop Med Hyg* **79:** 267–274. doi:10.4269/ajtmh.2008.79.267

Brackney DE, Isoe J, Black WC IV, Zamora J, Foy BD, Miesfeld RL, Olson KE. 2010. Expression profiling and comparative analyses of seven midgut serine proteases from the yellow fever mosquito, *Aedes aegypti*. *J Insect Physiol* **56:** 736–744. doi:10.1016/j.jinsphys.2010.01.003

Camacho C, Coulouris G, Avagyan V, Ma N, Papadopoulos J, Bealer K, Madden TL. 2009. BLAST+: architecture and applications. *BMC Bioinformatics* **10:** 421. doi:10.1186/1471-2105-10-421

Chan M, Johansson MA. 2012. The incubation periods of dengue viruses. *PLoS One* **7:** e50972. doi:10.1371/journal.pone.0050972

Chen Y, Lun AT, Smyth GK. 2016. From reads to genes to pathways: differential expression analysis of RNA-seq experiments using Rsubread and the edgeR quasi-likelihood pipeline. *F1000Res* **5:** 1438. doi:10.12688/f1000research.8987.2

Cui Y, Franz AWE. 2020. Heterogeneity of midgut cells and their differential responses to blood meal ingestion by the mosquito, *Aedes aegypti*. *Insect Biochem Mol Biol* **127:** 103496. doi:10.1016/j.ibmb.2020.103496

Devenport M, Alvarenga PH, Shao L, Fujioka H, Bianconi ML, Oliveira PL, Jacobs-Lorena M. 2006. Identification of the *Aedes aegypti* peritrophic matrix protein AeIMUCI as a heme-binding protein. *Biochemistry* **45:** 9540–9549. doi:10.1021/bi0605991

Dunkov BC, Georgieva T, Yoshiga T, Hall M, Law JH. 2002. *Aedes aegypti* ferritin heavy chain homologue: feeding of iron or blood influences message levels, lengths and subunit abundance. *J Insect Sci* **2:** 7. doi:10.1673/031.002.0701

Eggleston H, Adelman ZN. 2020. Transcriptomic analyses of *Aedes aegypti* cultured cells and ex vivo midguts in response to an excess or deficiency of heme: a quest for transcriptionally-regulated heme transporters. *BMC Genomics* **21:** 604. doi:10.1186/s12864-020-06981-5

Freyvogel TA, Staeubli W. 1965. The formation of the peritrophic membrane in Culicidae. *Acta Trop* **22:** 118–147.

Futschik ME, Carlisle B. 2005. Noise-robust soft clustering of gene expression time-course data. *J Bioinform Comput Biol* **3:** 965–988. doi:10.1142/S0219720005001375

Geiser DL, Chavez CA, Flores-Munguia R, Winzerling JJ, Pham DQ. 2003. *Aedes aegypti* ferritin. *Eur J Biochem* **270:** 3667–3674. doi:10.1046/j.1432-1033.2003.03709.x

Giraldo-Calderón GI, Emrich SJ, MacCallum RM, Maslen G, Dialynas E, Topalis P, Ho N, Gesing S, Madey G, Collins FH, et al. 2015. VectorBase: an updated bioinformatics resource for invertebrate vectors and other organisms related with human diseases. *Nucleic Acids Res* **43:** D707–D713. doi:10.1093/nar/gku1117

Harizanova N, Georgieva T, Dunkov BC, Yoshiga T, Law JH. 2005. *Aedes aegypti* transferrin. Gene structure, expression pattern, and regulation. *Insect Mol Biol* **14:** 79–88. doi:10.1111/j.1365-2583.2004.00533.x

Hixson B, Bing XL, Yang X, Bonfini A, Nagy P, Buchon N. 2022. A transcriptomic atlas of *Aedes aegypti* reveals detailed functional organization of

major body parts and gut regional specializations in sugar-fed and blood-fed adult females. *eLife* **11:** e76132. doi:10.7554/eLife.76132
Isoe J, Rascón AA Jr, Kunz S, Miesfeld RL. 2009. Molecular genetic analysis of midgut serine proteases in *Aedes aegypti* mosquitoes. *Insect Biochem Mol Biol* **39:** 903–912. doi:10.1016/j.ibmb.2009.10.008
Jiang Q, Hall M, Noriega FG, Wells M. 1997. cDNA cloning and pattern of expression of an adult, female-specific chymotrypsin from *Aedes aegypti* midgut. *Insect Biochem Mol Biol* **27:** 283–289. doi:10.1016/S0965-1748(97)00001-5
Kumar S, Molina-Cruz A, Gupta L, Rodrigues J, Barillas-Mury C. 2010. A peroxidase/dual oxidase system modulates midgut epithelial immunity in *Anopheles gambiae*. *Science* **327:** 1644–1648. doi:10.1126/science.1184008
Kuno G. 2010. Early history of laboratory breeding of *Aedes aegypti* (Diptera: Culicidae) focusing on the origins and use of selected strains. *J Med Entomol* **47:** 957–971. doi:10.1603/ME10152
Love MI, Huber W, Anders S. 2014. Moderated estimation of fold change and dispersion for RNA-seq data with DESeq2. *Genome Biol* **15:** 550. doi:10.1186/s13059-014-0550-8
Matthews BJ, Dudchenko O, Kingan SB, Koren S, Antoshechkin I, Crawford JE, Glassford WJ, Herre M, Redmond SN, Rose NH, et al. 2018. Improved reference genome of *Aedes aegypti* informs arbovirus vector control. *Nature* **563:** 501–507. doi:10.1038/s41586-018-0692-z
Molina-Cruz A, Gupta L, Richardson J, Bennett K, Black W IV, Barillas-Mury C. 2005. Effect of mosquito midgut trypsin activity on dengue-2 virus infection and dissemination in *Aedes aegypti*. *Am J Trop Med Hyg* **72:** 631–637. doi:10.4269/ajtmh.2005.72.631
Moreira LA, Edwards MJ, Adhami F, Jasinskiene N, James AA, Jacobs-Lorena M. 2000. Robust gut-specific gene expression in transgenic *Aedes aegypti* mosquitoes. *Proc Natl Acad Sci* **97:** 10895–10898. doi:10.1073/pnas.97.20.10895
Pertea M, Kim D, Pertea GM, Leek JT, Salzberg SL. 2016. Transcript-level expression analysis of RNA-seq experiments with HISAT, StringTie and ballgown. *Nat Protoc* **11:** 1650–1667. doi:10.1038/nprot.2016.095
Pham DQ-D, Chavez CA. 2005. The ferritin light-chain homologue promoter in *Aedes aegypti*. *Insect Mol Biol* **14:** 263–270. doi:10.1111/j.1365-2583.2005.00556.x
Pham DQD, Winzerling JJ. 2010. Insect ferritins: typical or atypical? *Biochim Biophys Acta* **1800:** 824–833. doi:10.1016/j.bbagen.2010.03.004
Pham DQ, Shaffer JJ, Chavez CA, Douglass PL. 2003. Identification and mapping of the promoter for the gene encoding the ferritin heavy-chain homologue of the yellow fever mosquito *Aedes aegypti*. *Insect Biochem Mol Biol* **33:** 51–62. doi:10.1016/S0965-1748(02)00167-4
Raquin V, Merkling SH, Gausson V, Moltini-Conclois I, Frangeul L, Varet H, Dillies MA, Saleh MC, Lambrechts L. 2017. Individual co-variation between viral RNA load and gene expression reveals novel host factors during early dengue virus infection of the *Aedes aegypti* midgut. *PLoS Negl Trop Dis* **11:** e0006152. doi:10.1371/journal.pntd.0006152
Rayms-Keller A, McGaw M, Oray C, Carlson JO, Beaty BJ. 2000. Molecular cloning and characterization of a metal responsive *Aedes aegypti* intestinal mucin cDNA. *Insect Mol Biol* **9:** 419–426. doi:10.1046/j.1365-2583.2000.00202.x
R Core Team. 2023. *R: a language and environment for statistical computing*. R Foundation for Statistical Computing, Vienna. https://www.R-project.org/
Rueden CT, Schindelin J, Hiner MC, DeZonia BE, Walter AE, Arena ET, Eliceiri KW. 2017. ImageJ2: ImageJ for the next generation of scientific image data. *BMC Bioinformatics* **18:** 529. doi:10.1186/s12859-017-1934-z
Sanders HR, Evans AM, Ross LS, Gill SS. 2003. Blood meal induces global changes in midgut gene expression in the disease vector, *Aedes aegypti*. *Insect Biochem Mol Biol* **33:** 1105–1122. doi:10.1016/S0965-1748(03)00124-3
Shao L, Devenport M, Fujioka H, Ghosh A, Jacobs-Lorena M. 2005. Identification and characterization of a novel peritrophic matrix protein, Ae-Aper50, and the microvillar membrane protein, AEG12, from the mosquito, *Aedes aegypti*. *Insect Biochem Mol Biol* **35:** 947–959. doi:10.1016/j.ibmb.2005.03.012
Stobbart RH. 1977. The control of the diuresis following a blood meal in females of the yellow fever mosquito *Aedes aegypti* (L). *J Exp Biol* **69:** 53–85. doi:10.1242/jeb.69.1.53
Tsujimoto H, Adelman ZN. 2021. Improved fecundity and fertility assay for *Aedes aegypti* using 24 well tissue culture plates (EAgaL plates). *J Vis Exp* **171:** e61232. doi:10.3791/61232
Tsujimoto H, Anderson MAE, Myles KM, Adelman ZN. 2018. Identification of candidate iron transporters from the ZIP/ZnT gene families in the mosquito *Aedes aegypti*. *Front Physiol* **9:** 380. doi:10.3389/fphys.2018.00380
Tsujimoto H, Anderson MAE, Eggleston H, Myles KM, Adelman ZN. 2021. *Aedes aegypti* dyspepsia encodes a novel member of the SLC16 family of transporters and is critical for reproductive fitness. *PLoS Negl Trop Dis* **15:** e0009334. doi:10.1371/journal.pntd.0009334
Wang Z, Zeng P, Zhou B. 2022. Identification and characterization of a heme exporter from the MRP family in *Drosophila melanogaster*. *BMC Biol* **20:** 126. doi:10.1186/s12915-022-01332-0
Whiten SR, Ray WK, Helm RF, Adelman ZN. 2018. Characterization of the adult *Aedes aegypti* early midgut peritrophic matrix proteome using LC-MS. *PLoS One* **13:** e0194734. doi:10.1371/journal.pone.0194734
WHO. 2009. *Dengue guidelines for diagnosis, treatment, prevention and control*, p. 160. World Health Organization, Geneva, Switzerland.
WHO. 2016. *Zika virus infection–United States of America–United States Virgin Islands*. World Health Organization, Geneva, Switzerland.
WHO. 2018. *A global strategy to eliminate yellow fever epidemics 2017–2026*. World Health Organization, Geneva, Switzerland.
WHO. 2019. *Zika epidemiology update*, pp. 1–13. World Health Organization, Geneva, Switzerland.
Ye J, Coulouris G, Zaretskaya I, Cutcutache I, Rozen S, Madden TL. 2012. Primer-BLAST: a tool to design target-specific primers for polymerase chain reaction. *BMC Bioinformatics* **13:** 134. doi:10.1186/1471-2105-13-134
Zhao B, Hou Y, Wang J, Kokoza VA, Saha TT, Wang XL, Lin L, Zou Z, Raikhel AS. 2016. Determination of juvenile hormone titers by means of LC-MS/MS/MS and a juvenile hormone-responsive Gal4/UAS system in *Aedes aegypti* mosquitoes. *Insect Biochem Mol Biol* **77:** 69–77. doi:10.1016/j.ibmb.2016.08.003
Zhou G, Velasquez LS, Geiser DL, Mayo JJ, Winzerling JJ. 2009. Differential regulation of transferrin 1 and 2 in *Aedes aegypti*. *Insect Biochem Mol Biol* **39:** 234–244. doi:10.1016/j.ibmb.2008.12.004
Zuker M. 2003. Mfold web server for nucleic acid folding and hybridization prediction. *Nucleic Acids Res* **31:** 3406–3415. doi:10.1093/nar/gkg595

Received February 16, 2023; accepted in revised form July 31, 2023.